



## JOULE HEATING EFFECT ON TERNARY NANOFLUID FLOW AND HEAT TRANSFER OVER A PERMEABLE CYLINDER

Umi Nadrah Hussein<sup>1</sup>, Najiyah Safwa Khashi'ie<sup>1,\*</sup>,  
Khairum Bin Hamzah<sup>2</sup>, Norihan Md Arifin<sup>3</sup> and Ioan Pop<sup>4</sup>

<sup>1</sup>Fakulti Teknologi dan Kejuruteraan Mekanikal  
Universiti Teknikal Malaysia Melaka  
Hang Tuah Jaya, 76100 Durian Tunggal  
Melaka, Malaysia

<sup>2</sup>Fakulti Teknologi dan Kejuruteraan Industri dan Pembuatan  
Universiti Teknikal Malaysia Melaka  
Hang Tuah Jaya, 76100 Durian Tunggal  
Melaka, Malaysia

<sup>3</sup>Department of Mathematics and Statistics  
Faculty of Science  
Universiti Putra Malaysia  
43400 UPM Serdang, Selangor, Malaysia

---

Received: August 27, 2024; Accepted: October 24, 2024

Keywords and phrases: dual solutions, Joule heating, magnetic field, shrinking cylinder, ternary nanofluid.

Communicated by K. K. Azad

---

How to cite this article: Umi Nadrah Hussein, Najiyah Safwa Khashi'ie, Khairum Bin Hamzah, Norihan Md Arifin and Ioan Pop, Joule heating effect on ternary nanofluid flow and heat transfer over a permeable cylinder, JP Journal of Heat and Mass Transfer 37(6) (2024), 831-841. <https://doi.org/10.17654/0973576324051>

This is an open access article under the CC BY license (<http://creativecommons.org/licenses/by/4.0/>).

Published Online: November 30, 2024

<sup>4</sup>Department of Mathematics  
Babeş-Bolyai University  
Cluj-Napoca, 400084, Romania

### **Abstract**

This study presents a comprehensive numerical investigation into the Joule heating effect on ternary nanofluid flow and heat transfer over a permeable cylinder. The nanofluid consists of copper, alumina, and titania nanoparticles suspended in a water base fluid. Key physical parameters, including magnetic field strength and suction, are incorporated into the model to assess their effects on the flow and thermal performance. The governing partial differential equations are transformed into ordinary differential equations via similarity transformation and solved using the `bvp4c` solver. The results are validated against previously published studies, showing excellent agreement. The analysis reveals that Joule heating significantly impacts the temperature distribution within the boundary layer, increasing its thickness. However, its influence on the skin friction coefficient and overall flow behavior remains minimal. These findings provide valuable insights into optimizing heat transfer and fluid flow in systems that utilize ternary nanofluids, with potential applications in advanced cooling technologies and industrial heat management systems.

### **1. Introduction**

Hybrid nanofluids represent an advanced class of nanofluids, created by dispersing two (hybrid) or three (ternary) types of nanoparticles within a base fluid. Numerous recent studies have explored the applications, benefits, and limitations of hybrid and ternary nanofluids, as well as their thermophysical characteristics (see Refs. [1-5]). Following this foundational work, a wide range of researchers have focused on the numerical analysis of hybrid nanofluid flow and heat transfer across different surfaces and conditions, utilizing the property correlations proposed by Devi and Devi [6] and Takabi and Salehi [7]. Recently, the flow of ternary hybrid nanofluids—fluids containing three distinct nanoparticles—has been extensively studied through

numerical analysis, particularly under the influence of various physical factors such as magnetic fields, velocity and thermal slips, heat absorption and generation, suction, among others. Jamrus et al. [8] discovered that increasing the volumetric concentration of titania in a copper-alumina-titania/water nanofluid model significantly enhanced the heat transfer rate. However, their study focused on stagnation point flow under mixed convection conditions. In another study, Jamrus et al. [9] explored a basic model and identified numerical dual solutions for the Hiemenz flow of ternary hybrid nanofluids over a stretching/shrinking sheet. They found that the ternary hybrid nanofluid (Cu-Al<sub>2</sub>O<sub>3</sub>-TiO<sub>2</sub>) exhibited higher skin friction and heat transfer coefficients compared to the binary hybrid nanofluid (Cu-Al<sub>2</sub>O<sub>3</sub>). Wahid et al. [10] found that a 4% increase in the suction parameter significantly extended the critical value, thereby delaying the boundary layer separation process.

These prior studies have motivated the authors to further expand the research by exploring (a) the existence of dual solutions and conducting stability analysis, and (b) examining the flow and heat transfer performance with varying parameter values. Consequently, this work focuses on the flow and heat transfer behavior of MHD ternary nanofluids (Cu-Al<sub>2</sub>O<sub>3</sub>-TiO<sub>2</sub>) over a shrinking/stretching cylinder, incorporating the effects of velocity slip and suction. Suction, in particular, plays a crucial role in stabilizing the reverse flow originating from the shrinking surface. The partial differential equations (PDEs) governing the system are converted into ordinary differential equations (ODEs) using the similarity transformation method. These transformed equations are then solved using the bvp4c solver. For validation, the numerical results are compared against previously published data under specific conditions. This study is both significant and valuable for future benchmarking, and the authors are confident that it offers potential for further extensions in subsequent research.

## 2. Mathematical Formulation

Consider a steady-state scenario involving the flow of a ternary hybrid nanofluid with heat transfer around a permeable cylinder of radius  $a$  as

depicted in Figure 1. The cylindrical coordinate system is chosen such that the  $x$ -axis runs along the cylinder's axis, while the  $r$ -axis represents the vertical direction and the flow occurs at  $r \geq 0$ . The velocity profile of the shrinking cylinder is described by  $\lambda U_w(x)$ , where  $U_w(x) = u_0 x/L$  and  $u_0$  is a constant. The ambient temperature is uniform,  $T_\infty$  while the variable temperature along the wall follows  $T_w = T_\infty + T_0(x/L)^2$ , where  $T_0$  is the characteristic temperature.

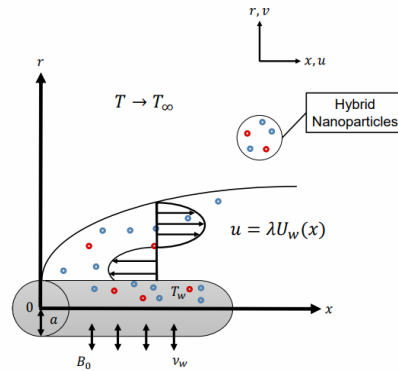


**Figure 1.** The physical model.

The governing partial differential equations (PDEs) which modeled the above physical flow are [8, 11]:

$$\frac{\partial u}{\partial x} + \frac{\partial v}{\partial r} = 0, \quad (1)$$

$$u \frac{\partial u}{\partial x} + v \frac{\partial u}{\partial r} = \frac{\mu_{thnf}}{\rho_{thnf}} \left( \frac{\partial^2 u}{\partial r^2} + \frac{1}{r} \frac{\partial u}{\partial r} \right) - \frac{\sigma_{thnf} B_0^2}{\rho_{thnf}} u, \quad (2)$$

$$u \frac{\partial T}{\partial x} + v \frac{\partial T}{\partial r} = \frac{k_{thnf}}{(\rho C_p)_{thnf}} \left( \frac{\partial^2 T}{\partial r^2} + \frac{1}{r} \frac{\partial T}{\partial r} \right) + \frac{\sigma_{thnf} B_0^2}{(\rho C_p)_{thnf}} u^2, \quad (3)$$

subject to the boundary conditions (BCs) [8, 11]:

$$\begin{aligned} u &= \lambda U_w, \quad v = v_w, \quad T = T_w, \quad \text{at } r = a, \\ u &\rightarrow 0, \quad T \rightarrow T_\infty, \quad \text{as } r \rightarrow \infty. \end{aligned} \quad (4)$$

In this model,  $u$  and  $v$  represent the velocity components along the  $x$ -axis and  $y$ -axis, respectively. The parameter  $\lambda$  governs the surface condition, where a negative value of  $\lambda$  indicates shrinking, a positive value corresponds to stretching, and  $\lambda = 0$  reflects a stationary surface. Table 1 details the thermophysical characteristics of both the hybrid and ternary hybrid nanofluids. The concentrations of alumina, copper, and titania are denoted as  $\phi_1$ ,  $\phi_2$  and  $\phi_3$ , respectively. The physical properties of the nanoparticles and base fluid are presented in Table 2. The appropriate similarity variables that satisfy the continuity equation (1) are as follows:

$$u = \frac{u_0 x f'(\eta)}{L}, v = -\frac{af(\eta)}{r} \sqrt{\frac{u_0 v_f}{L}}, \eta = \frac{r^2 - a^2}{2a} \sqrt{\frac{u_0}{v_f L}}, \theta(\eta) = \frac{T - T_\infty}{T_w - T_\infty}. \quad (5)$$

This setup ensures that the continuity equation is fulfilled while facilitating the analysis of the system. This process leverages the similarity transformation, which reduces the complexity of the system and simplifies the governing PDEs into a set of ordinary differential equations (ODEs). These ODEs are more manageable and allow for numerical or analytical solutions under appropriate boundary conditions, as demonstrated in previous studies [8, 11]. By substituting equation (5) into equations (1)-(4), the equations are reduced to:

$$\frac{\mu_{thnf}/\mu_f}{\rho_{thnf}/\rho_f} [(1 + 2\eta\gamma) f''' + 2\gamma f''] + ff'' - f'^2 - \frac{\sigma_{thnf}/\sigma_f}{\rho_{thnf}/\rho_f} Mf' = 0, \quad (6)$$

$$\frac{1}{Pr} \frac{k_{thnf}/k_f}{(\rho C_p)_{thnf}/(\rho C_p)_f} [(1 + 2\gamma\eta)\theta'' + 2\gamma\theta'] + f\theta' - 2f'\theta + \frac{\sigma_{thnf}/\sigma_f}{(\rho C_p)_{thnf}/(\rho C_p)_f} EcMf'^2 = 0, \quad (7)$$

$$f(0) = S, f'(0) = \lambda, \theta(0) = 1,$$

$$f'(\eta) \rightarrow 0, \theta(\eta) \rightarrow 0 \text{ as } \eta \rightarrow \infty. \quad (8)$$

The parameters in equations (6)-(8) are defined as the magnetic parameter ( $M = \sigma_f L B_0^2 / \rho_f u_0$ ), Prandtl number ( $Pr = (\mu C_p)_f / k_f$ ) and Eckert number

( $Ec = U_w^2/(C_p)_f(T_w(x) - T_\infty)$ ). The key physical quantities of interest are the skin friction coefficient and the rate of heat transfer at the surface, which help evaluate the behavior of the flow and heat transfer around the cylinder and are essential in characterizing the performance of the system. They can be expressed as follows [11]:

$$Re_x^{1/2} C_f = \frac{\mu_{thnf}}{\mu_f} f''(0), \quad Re_x^{-1/2} Nu_x = -\frac{k_{thnf}}{k_f} \theta'(0), \quad (9)$$

where  $Re_x = U_w(x)x/\nu_f$  (local Reynolds number).

**Table 1.** Correlations of ternary hybrid nanofluid

Properties	Hybrid Nanofluid (hnf) and Ternary Hybrid Nanofluid (thnf)
Density	$\rho_{thnf} = (1 - \phi_3) \{ (1 - \phi_2) [(1 - \phi_1) \rho_f + \phi_1 \rho_{s1}] + \phi_2 \rho_{s2} \} + \phi_3 \rho_{s3}$
Heat capacity	$(\rho C_p)_{thnf} = (1 - \phi_3) \left\{ (1 - \phi_2) \left[ (1 - \phi_1) (\rho C_p)_f \right] + \phi_1 (\rho C_p)_{s1} \right\} + \phi_2 (\rho C_p)_{s2} + \phi_3 (\rho C_p)_{s3}$
Dynamic viscosity	$\frac{\mu_{thnf}}{\mu_f} = \frac{1}{(1 - \phi_1)^{2.5} (1 - \phi_2)^{2.5} (1 - \phi_3)^{2.5}}$
Thermal conductivity	$\frac{k_{thnf}}{k_{hnf}} = \left[ \frac{k_{s3} + 2k_{hnf} - 2\phi_3(k_{hnf} - k_{s3})}{k_{s3} + 2k_{hnf} + \phi_3(k_{hnf} - k_{s3})} \right],$ <p>where</p> $\frac{k_{hnf}}{k_{nf}} = \left[ \frac{k_{s2} + 2k_{nf} - 2\phi_2(k_{nf} - k_{s2})}{k_{s2} + 2k_{nf} + \phi_2(k_{nf} - k_{s2})} \right]$ $\frac{k_{nf}}{k_f} = \left[ \frac{k_{s1} + 2k_f - 2\phi_1(k_f - k_{s1})}{k_{s1} + 2k_f + \phi_1(k_f - k_{s1})} \right]$
Electrical conductivity	$\frac{\sigma_{thnf}}{\sigma_{hnf}} = \left[ \frac{\sigma_{s3} + 2\sigma_{hnf} - 2\phi_3(\sigma_{hnf} - \sigma_{s3})}{\sigma_{s3} + 2\sigma_{hnf} + \phi_3(\sigma_{hnf} - \sigma_{s3})} \right],$ <p>where</p> $\frac{\sigma_{hnf}}{\sigma_{nf}} = \left[ \frac{\sigma_{s2} + 2\sigma_{nf} - 2\phi_2(\sigma_{nf} - \sigma_{s2})}{\sigma_{s2} + 2\sigma_{nf} + \phi_2(\sigma_{nf} - \sigma_{s2})} \right]$ $\frac{\sigma_{nf}}{\sigma_f} = \left[ \frac{\sigma_{s1} + 2\sigma_f - 2\phi_1(\sigma_f - \sigma_{s1})}{\sigma_{s1} + 2\sigma_f + \phi_1(\sigma_f - \sigma_{s1})} \right]$

**Table 2.** Thermophysical properties for Cu, H<sub>2</sub>O and Al<sub>2</sub>O<sub>3</sub>

Physical properties	Cu	Al <sub>2</sub> O <sub>3</sub>	TiO <sub>2</sub>	Water
$\rho(\text{kg/m}^3)$	8933	3970	4250	997.1
$C_p(\text{J/kgK})$	385	765	686.2	4179
$k(\text{W/mK})$	400	40	8.9538	0.6130
$\sigma(\text{s/m})$	$59.6 \times 10^6$	$35 \times 10^6$	$2.6 \times 10^6$	$5.5 \times 10^6$

### 3. Results and Discussion

The numerical solutions for the reduced ODEs from the prior section were solved using Matlab's `bvp4c` function. The computed results, displayed in the accompanying figures and tables, show the heat transfer and skin friction coefficients for the ternary copper-alumina-titania nanofluid flow under selected conditions. As demonstrated in Table 3, the obtained data agrees well with previous research, validating the current model's effectiveness. This consistency indicates the model's potential for generating additional results in tables and figures across various parameter ranges.

**Table 3.** Model validation of  $f''(0)$  with limitations  $\lambda = 1$ ,  $\text{Pr} = 6.2$ ,  $\phi_2 = \phi_3 = \gamma = M = Ec = S = 0$  and various  $\phi_1$ 

$\phi_1$	$f''(0)$		
	Present	Waini et al. [12]	Jamrus et al. [13]
0.05	-1.00538	-1.00538	-1.00538
0.10	-0.99877	-0.99877	-0.99877
0.15	-0.98184	-0.98184	-0.98185
0.20	-0.95592	-0.95592	-0.95593

Figure 2 demonstrates the emergence of boundary layer separation within the shrinking (opposing) flow region when the Eckert numbers ( $Ec$ ) are varied. The analysis shows that increasing Eckert number does not delay the onset of boundary layer separation (not affecting the separation point). In this work, the obtained separation point/critical value/endpoint is  $\lambda_c = -1.0375$  and same for all Eckert numbers ( $Ec = 0, 0.01, 0.02$ ). As illustrated in Figure 2, an increase in  $Ec$  leads to a reduction in the heat

transfer rate. Physically, when the  $Ec$  increases, it signifies that a greater proportion of the kinetic energy in the flow is converted into internal energy (heat) due to viscous dissipation. This dissipation heats the fluid within the boundary layer, which reduces the temperature gradient between the surface of the shrinking cylinder and the fluid. Since heat transfer is driven by the temperature gradient, a reduced gradient leads to a lower rate of heat transfer from the cylinder's surface to the surrounding fluid. In the context of a shrinking cylinder, where the flow is already adverse and prone to separation, the additional heating caused by viscous dissipation (as represented by the  $Ec$ ) further reduces the cooling effect. This results in less efficient heat removal from the surface, and thus, the overall heat transfer rate declines. The increasing  $Ec$  reduces the heat transfer rate because higher viscous dissipation reduces the temperature gradient driving the thermal energy exchange between the surface and the surrounding fluid.

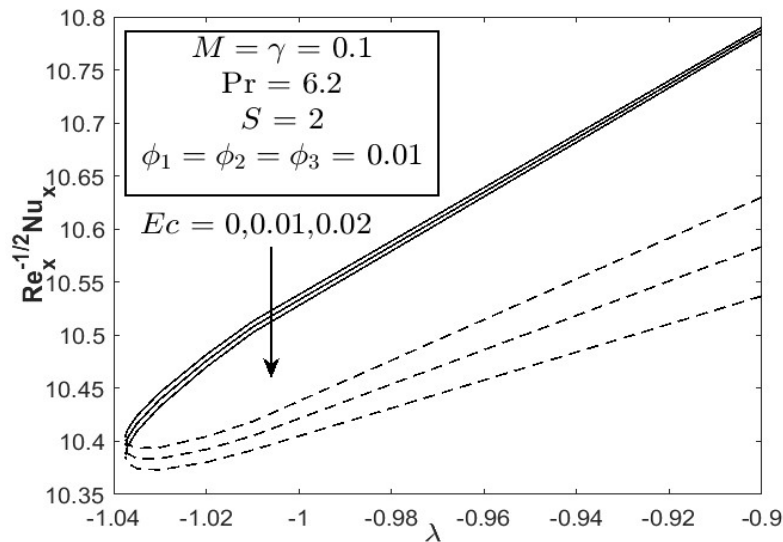


**Figure 2.** Effect of Eckert number (Joule heating) on the heat transfer rate.

#### 4. Conclusions

This study presents a comprehensive numerical investigation of the Joule heating effect on ternary nanofluid flow and heat transfer over a permeable



cylinder. Using a combination of copper, alumina, and titania nanoparticles dispersed in water, the analysis explored key physical parameters, including the effects of magnetic fields, velocity slip, and suction on the flow behavior and thermal performance. The main findings of the study indicate that:

**Joule heating impact.** The inclusion of Joule heating significantly affects the temperature distribution in the boundary layer, leading to an increase in the thermal boundary layer thickness. However, its effect on the overall flow behavior and skin friction is minimal.

**Suction and permeability.** The application of suction over the permeable cylinder effectively stabilizes the boundary layer and delays the onset of separation. Higher suction values result in an enhanced heat transfer rate and improved flow stability.

This study adds valuable insights into the behavior of ternary nanofluids in complex flow and heat transfer scenarios. The findings have implications for the design of cooling systems and industrial applications where precise thermal management is required. Future research could further explore the effect of additional physical parameters such as non-uniform magnetic fields, higher nanoparticle concentrations, or more advanced thermal boundary conditions to optimize nanofluid performance in real-world applications.

### Acknowledgement

We appreciate the research and financial supports from Universiti Teknikal Malaysia Melaka through grant JURNAL/2022/FTKM/Q00087.

### References

- [1] H. Adun, D. Kavaz and M. Dagbasi, Review of ternary hybrid nanofluid: Synthesis, stability, thermophysical properties, heat transfer applications, and environmental effects, *Journal of Cleaner Production* 328 (2021), 129525.
- [2] J. Mohammed Zayan, A. K. Rasheed, A. John, M. Khalid, A. F. Ismail, A. Aabid and M. Baig, Investigation on rheological properties of water-based novel ternary

- hybrid nanofluids using experimental and Taguchi method, *Materials* 15(1) (2021), 28.
- [3] H. Babar and H. M. Ali, Towards hybrid nanofluids: preparation, thermophysical properties, applications, and challenges, *Journal of Molecular Liquids* 281 (2019), 598-633.
- [4] M. Mahboobtosi, K. Hosseinzadeh and D. D. Ganji, Investigating the convective flow of ternary hybrid nanofluids and single nanofluids around a stretched cylinder: Parameter analysis and performance enhancement, *International Journal of Thermofluids* 23 (2024), 100752.
- [5] H. Adun, M. Adedeji, M. Dagbasi and A. Babatunde, Amelioration of thermodynamic performance and environmental analysis of an integrated solar power generation system with storage capacities using optimized ternary hybrid nanofluids, *Journal of Energy Storage* 51 (2022), 104531.
- [6] S. S. A. Devi and S. S. U. Devi, Numerical investigation of hydromagnetic hybrid Cu-Al<sub>2</sub>O<sub>3</sub>/water nanofluid flow over a permeable stretching sheet with suction, *International Journal of Nonlinear Sciences and Numerical Simulation* 17(5) (2016), 249-257.
- [7] B. Takabi and S. Salehi, Augmentation of the heat transfer performance of a sinusoidal corrugated enclosure by employing hybrid nanofluid, *Advances in Mechanical Engineering* 6 (2014), 147059.
- [8] F. N. Jamrus, I. Waini, U. Khan and A. Ishak, Effects of magnetohydrodynamics and velocity slip on mixed convective flow of thermally stratified ternary hybrid nanofluid over a stretching/shrinking sheet, *Case Studies in Thermal Engineering* 55 (2024), 104161.
- [9] F. N. Jamrus, A. Ishak, I. Waini, U. Khan, M. I. H. Siddiqui and J. K. Madhukesh, Aspects of non-unique solutions for Hiemenz flow filled with ternary hybrid nanofluid over a stretching/shrinking sheet, *Advances in Mathematical Physics* 2024(1) (2024), 7253630.
- [10] N. S. Wahid, N. M. Arifin, R. I. Yahaya, N. S. Khashi'ie and I. Pop, Impact of suction and thermal radiation on unsteady ternary hybrid nanofluid flow over a biaxial shrinking sheet, *Alexandria Engineering Journal* 96 (2024), 132-141.
- [11] N. S. Khashi'ie, N. M. Arifin, I. Pop and N. S. Wahid, Flow and heat transfer of hybrid nanofluid over a permeable shrinking cylinder with Joule heating: A comparative analysis, *Alexandria Engineering Journal* 59(3) (2020), 1787-1798.
- [12] I. Waini, F. N. Jamrus, A. R. M. Kasim, A. Ishak and I. Pop, Homogeneous-heterogeneous reactions on Al<sub>2</sub>O<sub>3</sub>-Cu hybrid nanofluid flow over a shrinking

sheet, *Journal of Advanced Research in Fluid Mechanics and Thermal Sciences* 102(1) (2023), 85-97.

- [13] F. N. Jamrus, I. Waini and A. Ishak, Time-depending flow of ternary hybrid nanofluid past a stretching sheet with suction and magnetohydrodynamic (MHD) effects, *Journal of Advanced Research in Fluid Mechanics and Thermal Sciences* 117(2) (2024), 15-27.